Supplement of

A Comparative Study to Reveal the Influence of Typhoons on the Transport, Production and Accumulation of O_3 in the Pearl River Delta, China

Kun Qu[1,2], Xuesong Wang[1,2], Yu Yan[1,2], Jin Shen[3], Teng Xiao[1,2], Huabin Dong[1,2], Limin Zeng[1,2], and Yuanhang Zhang[1,2,4,5]

[1]State Key Joint Laboratory of Environmental Simulation and Pollution Control, College of Environmental Sciences and Engineering, Peking University, Beijing 100871, China
[2]International Joint Laboratory for Regional Pollution Control, Ministry of Education, Beijing, 100816, China
[3]State Key Laboratory of Regional Air Quality Monitoring, Guangdong Key Laboratory of Secondary Air Pollution Research, Guangdong Environmental Monitoring Center, Guangzhou 510308, China
[4]Beijing Innovation Center for Engineering Science and Advanced Technology, Peking University, Beijing 100871, China
[5]CAS Center for Excellence in Regional Atmospheric Environment, Chinese Academy of Sciences, Xiamen 361021, China
Correspondence to: Xuesong Wang (xswang@pku.edu.cn) and Yuanhang Zhang (yhzhang@pku.edu.cn)

1. Evaluation of WRF and CMAQ modelling results within the PRD

The WRF-modelling results of air temperature, relative humidity (RH), zonal and meridional wind speeds in the PRD were evaluated based on the same-period routine monitoring datasets collected in 29 national meteorological sites (Fig. S1a). Statistics listed in Table S4 indicate low biases and high correlations between the modelled and observational series of air temperature and RH. Wind speeds in two directions were overall overestimated by 0.6–0.8 m/s, but it was normally found in the PRD modelling studies (Chen et al, 2018; Deng et al, 2018; Tse et al, 2018; Yuan et al, 2018). Low modelling resolution, as well as coarse descriptions of surface features might contribute to these biases. High R values (>0.8) of wind speeds, especially meridional wind speeds, suggest that the model was capable of describing the variation of wind fields within the PRD. Acceptable performance in the WRF modelling ensures the validity of the meteorological inputs for the CMAQ modelling.

The comparisons of observational and modelling mean O_3 MDA8 and daily NO_2 concentrations in 18 sites of the Guangzhou-Hong Kong-Macao regional monitoring network (Fig. S1b) in the two represented months are shown in Fig. S10a–d. High FAC2 and R, low NMB indicate good performance in the modelling of these two species. We also evaluated the performance of the daily mixing ratios of non-methane hydrocarbons (NMHCs) based on the GC/MS measurements in five representative sites within the PRD (Zhudong, Modiesha, Heshan Supersite, Xijiao and Daxuecheng, locations shown in Fig. S1b), which is overall satisfying, as well (Fig. S10e–f). Note that the notable overestimations of NO_2 and NMHCs levels can be found during 11–13 July, when the PRD was under the influence of heavy rainfall. Since these days were classified as clean days and were excluded in comparisons, it did not affect the final conclusions.

2. Tables

Table S1. Information on the O_3 pollution days in October, 2014–2018.

Date	Number of Days	Classification	Weather systems
October 2–3, 2014	2	Autumn, typhoon-induced	The typhoon Phanfone
October 5, 2014	1	Autumn, typhoon-induced	The typhoon Phanfone & Vongfong
October 7–11, 2014	5	Autumn, typhoon-induced	The typhoon Vongfong
October 14–16, 2015	3	Autumn, typhoon-induced	The typhoon Koppu & Champi
October 21, 2015	1	Autumn, typhoon-induced	The typhoon Champi
October 4, 2016	1	Autumn, typhoon-induced	The typhoon Chaba & Aere
October 14, 2016	1	Autumn, typhoon-induced	The typhoon Sarika
October 11, 2017	1	Autumn, typhoon-induced	The typhoon Khanum
October 18, 2017	1	Autumn, typhoon-induced	The typhoon Lan
October 22, 2017	1	Autumn, typhoon-induced	The typhoon Lan & Saola
October 25–29. 2017	5	Autumn, typhoon-induced	The typhoon Saola
October 1–3, 2018 October 5–6, 2018	5	Autumn, typhoon-induced	The typhoon Kong-rey
October 27–29, 2018	3	Autumn, typhoon-induced	The typhoon Yutu
October 17–19, 2015	3	Autumn, close typhoon-induced	The typhoon Koppu & Champi
October 5–6, 2016	2	Autumn, close typhoon-induced	The typhoon Chaba & Aere
October 10, 2016	1	Autumn, close typhoon-induced	The typhoon Aere & Songda
October 20, 2016	1	Autumn, close typhoon-induced	The typhoon Haima
October 12–13, 2017	2	Autumn, close typhoon-induced	The typhoon Khanum
October 4, 2018	1	Autumn, close typhoon-induced	The typhoon Kong-rey
October 1, 2014	1	Autumn, far typhoon-induced	The typhoon Phanfone
October 6, 2014	1	Autumn, far typhoon-induced	The typhoon Phanfone & Vongfong
October 13, 2015	1	Autumn, far typhoon-induced	The typhoon Koppu & Champi
October 22–25, 2015	4	Autumn, far typhoon-induced	The typhoon Champi
October 23–24, 2017	2	Autumn, far typhoon-induced	The typhoon Lan & Saola
October 14–21, 2014	8	Autumn, no-typhoon	Subtropical high
October 15–31, 2014	7	Autumn, no-typhoon	Subtropical high
October 9, 2015	1	Autumn, no-typhoon	Continental cold high
October 28, 2015	1	Autumn, no-typhoon	Subtropical high
October 27–28, 2016	2	Autumn, no-typhoon	Foreside of a cold front
October 31, 2016	1	Autumn, no-typhoon	Subtropical high
October 6–8, 2017	3	Autumn, no-typhoon	Subtropical high
October 30–31, 2017	2	Autumn, no-typhoon	Sea high
October 7–9, 2018	3	Autumn, no-typhoon	Foreside of a cold front
October 12, 2018	1	Autumn, no-typhoon	Sea high

Table S2. Information on the O_3 pollution days in July, 2014–2018.

Date	Number of Days	Classification	Weather systems
July 6–9, 2014	4	Summer, typhoon-induced	The typhoon Neoguri
July 16–17, 2014	2	Summer, typhoon-induced	The typhoon Rammasun
July 21–25, 2014	5	Summer, typhoon-induced	The typhoon Matmo
July 29–31, 2014	3	Summer, typhoon-induced	The typhoon Nakri & Halong
July 11–12, 2015	2	Summer, typhoon-induced	The typhoon Chan-hom & Nangka
July 7–8, 2016	2	Summer, typhoon-induced	The typhoon Nepartak
July 30-31, 2016	2	Summer, typhoon-induced	The typhoon Nida
July 25–27, 2017	3	Summer, typhoon-induced	The typhoon Nesat & Noru
July 10, 2018	1	Summer, typhoon-induced	The typhoon Maria
July 9, 2016	1	Summer, close typhoon-induced	The typhoon Nepartak
July 22, 2017	1	Summer, close typhoon-induced	The typhoon Roke
July 28–31, 2017	4	Summer, close typhoon-induced	The typhoon Nesat, Noru & Haitang
July 11, 2017	1	Summer, close typhoon-induced	The typhoon Maria
July 17, 2017	1	Summer, close typhoon-induced	The typhoon Son-tinh
July 13–16, 2015	4	Summer, far typhoon-induced	The typhoon Nangka
July 8, 2018	1	Summer, far typhoon-induced	The typhoon Maria
July 28–29, 2018	2	Summer, far typhoon-induced	The typhoon Jongdari
July 10, 2016	1	\	The typhoon Nepartak*
July 12, 2018	1	\	The typhoon Maria**
July 19–22, 2018	4	\	The typhoon Son-tinh & Ampil**
July 28, 2014	1	Summer, no-typhoon	Subtropical high
July 31, 2015	1	Summer, no-typhoon	Subtropical high
July 22–26, 2016	5	Summer, no-typhoon	Subtropical high
July 29, 2016	1	Summer, no-typhoon	Subtropical high
July 13, 2017	1	Summer, no-typhoon	Subtropical high
July 20, 2017	1	Summer, no-typhoon	Subtropical high

* No typhoon record at 14:00 LT.
** Typhoons located to the west of the PRD.

Table S3. The numbers, proportions of O_3 pollution days, and O_3 concentrations in each month.

Parameters	October 2014	October 2015	October 2016	October 2017	October 2018	July 2014	July 2015	July 2016	July 2017	July 2018
Number of O_3 pollution days	25	14	9	17	13	15	7	12	10	11
With typhoons	10	12	6	12	9	14	6	6	8	11
Typhoon-induced days	8	4	2	8	8	14	2	4	3	5
Without typhoons (no-typhoon days)	15	2	3	5	4	1	1	6	2	0
Mean PRD-max O_3 MDA8 ($\mu g/m^3$)										
Typhoon-induced days	199.4	221.2	149.9	200.1	200.7	209.4	184.1	246.3	202.9	171.6
No-typhoon days	190.7	174.7	167.6	189.4	211.4	220.0	140.4	206.0	140.9	/
Mean PRD-max O_3 MDA1 ($\mu g/m^3$)										
Typhoon-induced days	230.1	261.5	207.0	239.1	230.1	272.4	213.5	302.5	242.3	220.8
No-typhoon days	234.5	219.0	220.0	219.6	250.0	253.0	240.0	256.5	216.5	/

Table S4. Statistics of the WRF modelling performance of air temperature, RH, zonal and meridional wind speeds in October 2015 and July 2016.

Parameters	Statistics	October 2015	July 2016
Air Temperature	MB* (K)	-0.46	0.03
	RMSE** (K)	0.86	1.27
	R***	0.98	0.90
Relative Humidity	MB (%)	-3.13	-5.29
	RMSE (%)	5.01	8.11
	R	0.96	0.90
Zonal Wind Speed	MB (m/s)	-0.72	-0.17
	RMSE (m/s)	0.82	0.74
	R	0.78	0.89
Meridional Wind Speed	MB (m/s)	-0.62	0.77
	RMSE (m/s)	1.05	1.11
	R	0.93	0.91

* MB, mean bias.
** RMSE, root-mean-square error.
*** R, correlation factor.

3. Figures

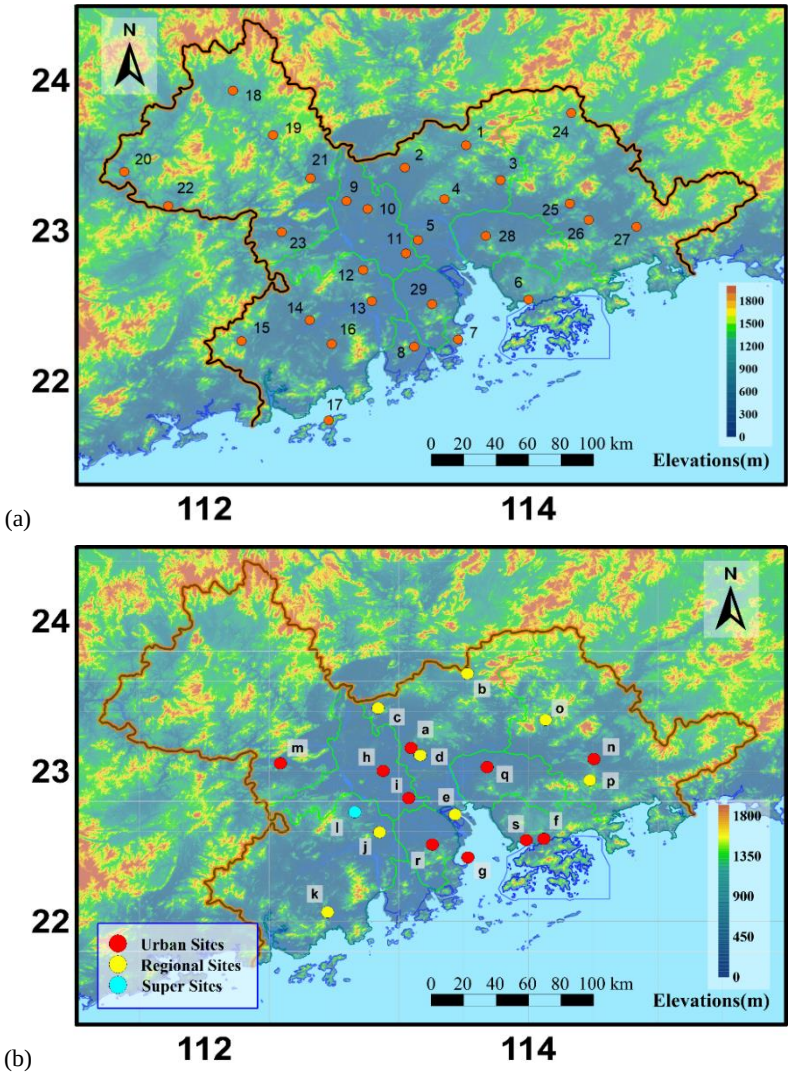

Figure S1. (a) The spatial distribution of 29 national meteorological sites within the PRD: 1. Conghua; 2. Huadu; 3. Zengcheng; 4. Huangpu; 5. Panyu; 6. Shenzhen; 7. Zhuhai; 8. Doumen; 9. Sanshui; 10. Nanhai; 11. Shunde; 12. Heshan; 13. Xinhui; 14. Kaiping; 15. Enping; 16. Taishan; 17. Shangchuandao; 18. Huaiji; 19. Guangning; 20. Fengkai; 21. Sihui; 22. Deqing; 23. Gaoyao; 24. Longmen; 25. Boluo; 26. Huiyang; 27. Huidong; 28. Dongguan; 29. Zhongshan.
(b) The spatial distribution of the sites of the Guangdong-Hong Kong-Macao regional monitoring network (the site a–r) and the GC/MS measurements (the site c, d, l, o, s): a. Luhu; b. Tianhu; c. Zhudong; d. Modiesha; e. Wanqingsha; f. Liyuan; g. Tangjia; h. Huijingcheng; i. Jinjuju; j. Donghu; k. Duanfen; l. Heshan Supersite; m. Chengzhongzizhan; n. Xiapu; o. Xijiao; p. Jinguowan; q. Nanchengyuanling; r. Zimaling; s. Daxuecheng.

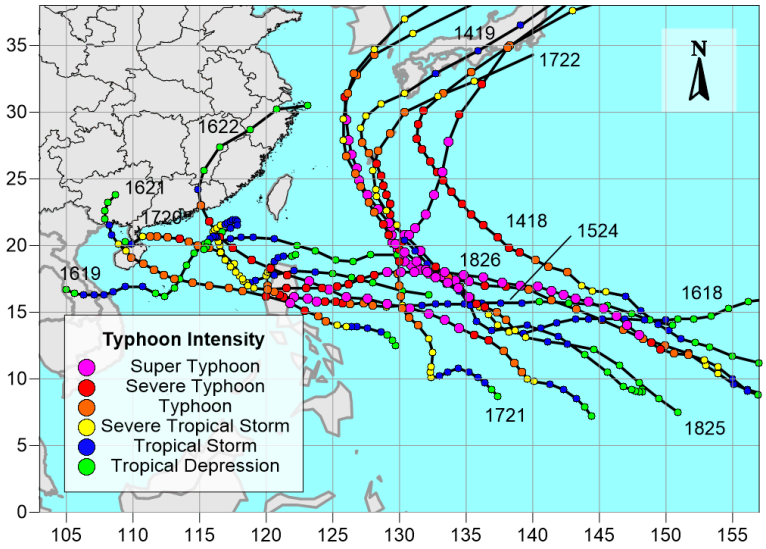

Figure S2. The tracks of typhoons related to O_3 pollution in the PRD in October, 2014–2018. The 4-digit identification numbers of all typhoons are also shown in plot.

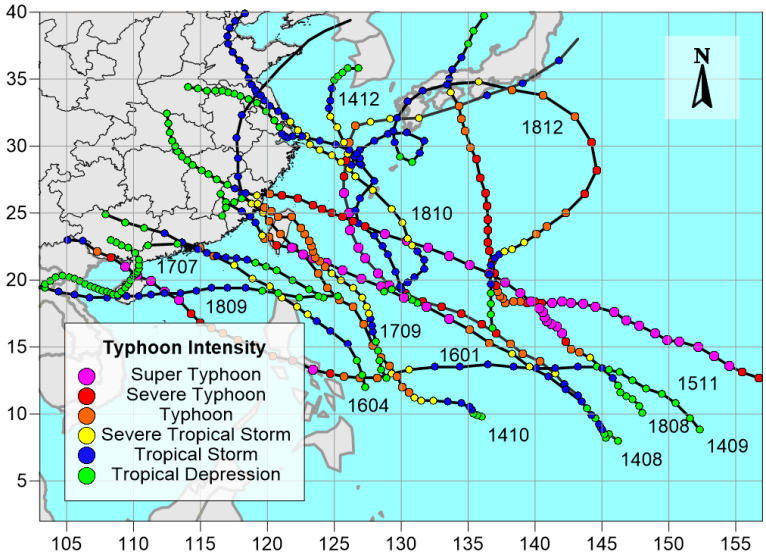

Figure S3. The tracks of typhoons related to O_3 pollution in the PRD in July, 2014–2018. The 4-digit identification numbers of all typhoons are also shown in plot.

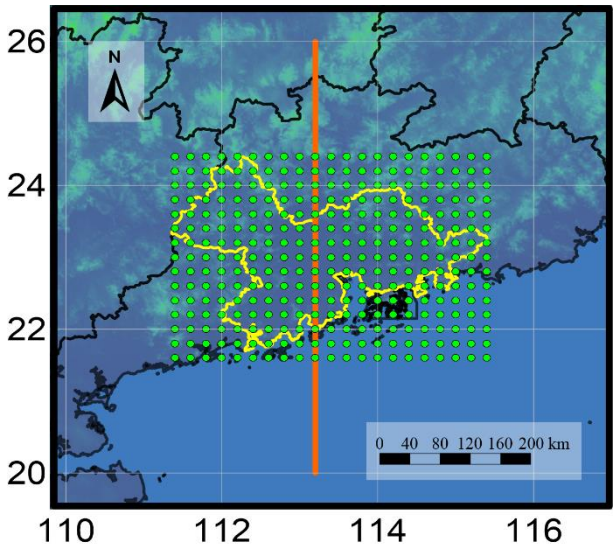

Figure S4. Geographical information used in this study: (1) the matrix of starting points (green) and the boarder of the PRD (yellow) in the calculation of APRTs; (2) the cross section was made along the orange line (from 26.0 ℕ to 20.0 ℕ along the 113.2 ℇ longitude line).

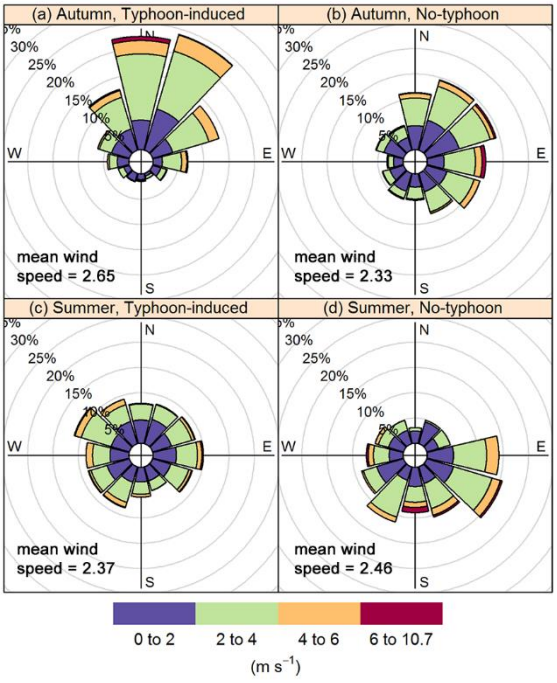

Figure S5. Wind roses at 14:00 LT in four scenarios: (a) autumn, typhoon-induced; (b) autumn, no-typhoon; (c) summer, typhoon-induced; (d) summer, no-typhoon. The routine monitoring data collected in 29 meteorological sites within the PRD were used.

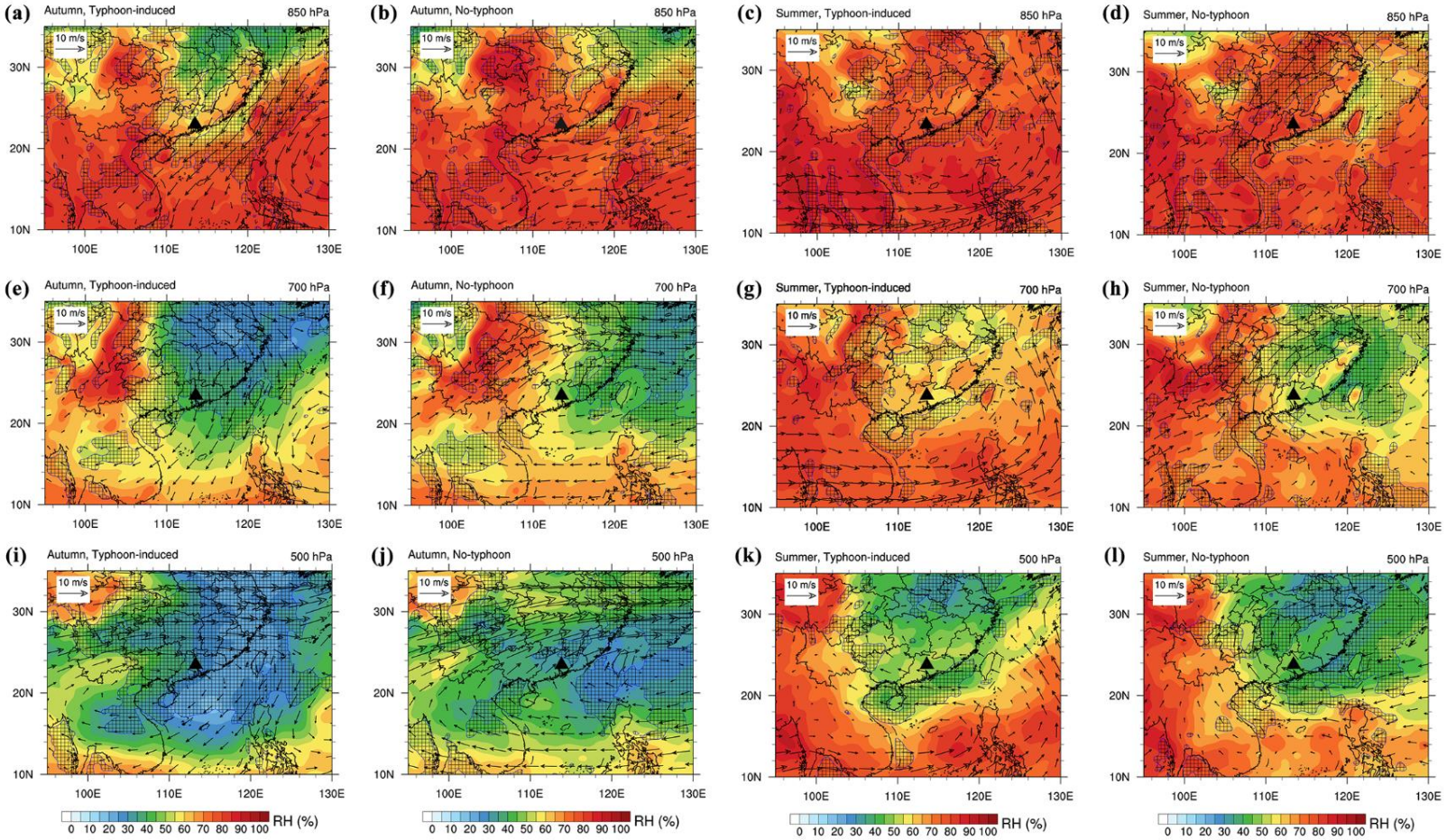

Figure S6. Relative humidity (%) and wind fields at the height of (a–d) 850 hPa, (e–h) 700 hPa, and (i–l) 500 hPa at 14:00 LT for the four scenarios: (a, e, i) autumn, typhoon-induced; (b, f, j) autumn, no-typhoon; (c, g, k) summer, typhoon-induced; and (d, h, l) summer, no-typhoon. The black triangle in each plot indicates the PRD. The gridded areas indicate that vertical wind speed is less than 0, or downdrafts occur.

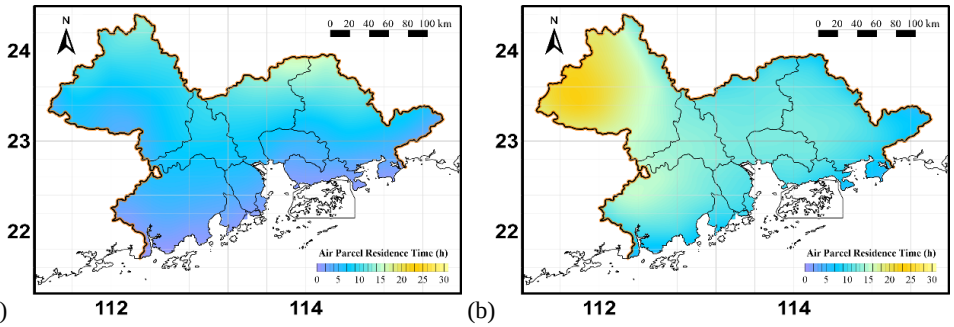

Figure S7. The spatial distributions of APRTs in the PRD for the close typhoon-scenarios of (a) autumn and (b) summer.

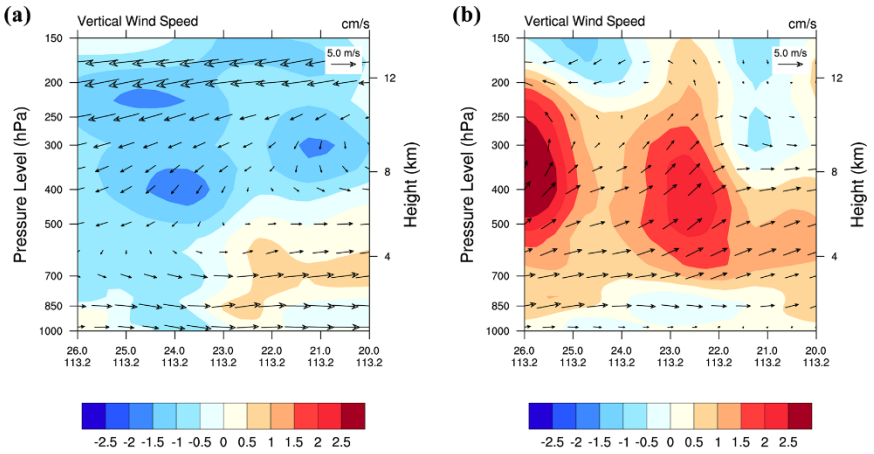

Figure S8. The cross section of mean vertical wind field at 14:00 LT for the close typhoon-induced scenario of (a) autumn and (b) summer. Cross sections are made from 26.0 ℃N to 20.0 ℃N along the 113.2 ℃E longitude line (Fig. S4). The vectors indicate meridional wind speed (m/s) and vertical wind speed (cm/s), and the contours indicate vertical wind speed (cm/s).

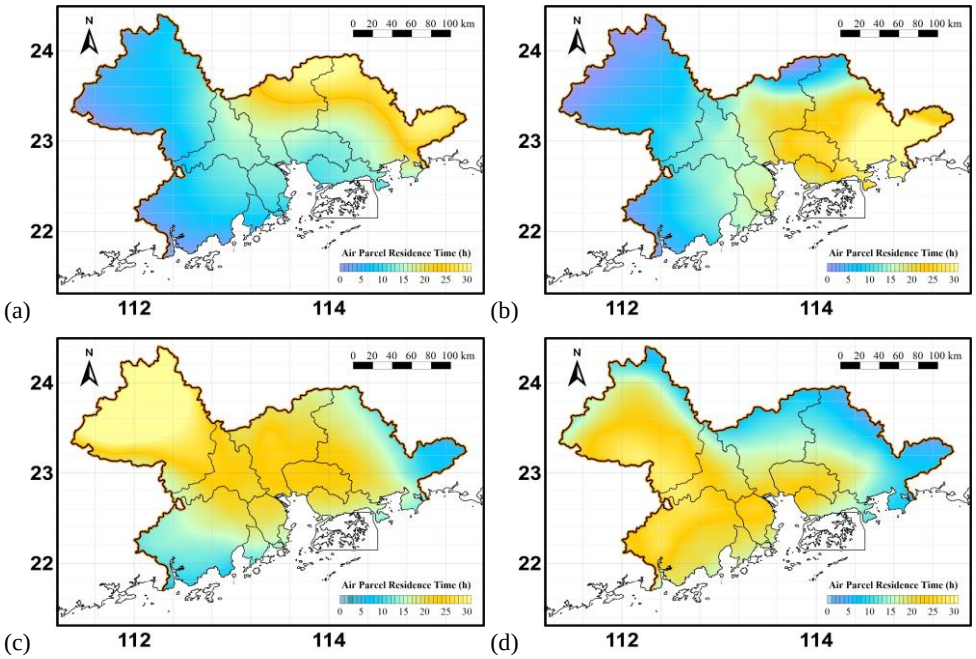

Figure S9. The spatial distributions of APRTs in the PRD on the representative O_3 pollution days: (a) the typhoon-induced days in October 2015 (14–16 and 21 October 2015); (b) the no-typhoon days in October 2015 (28 October and 3–5 November 2015); (c) the typhoon-induced days in July 2016 (7–8 and 30–31 July 2016); and (d) the no-typhoon days in July 2016 (22–26 and 29 July 2016).

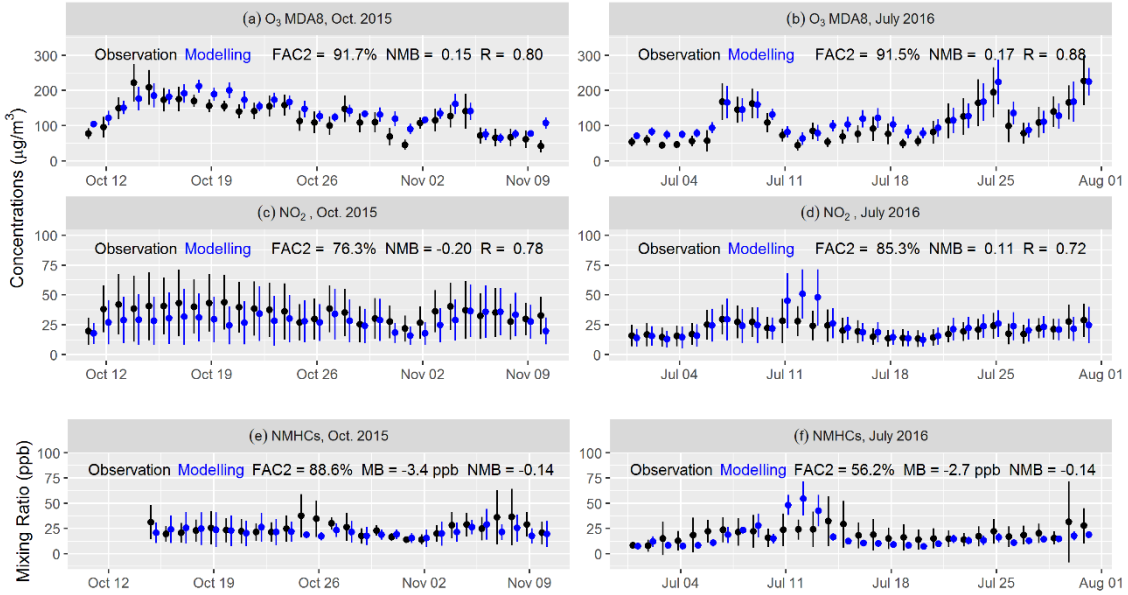

Figure S10. Comparisons between the observational and modelling mean O_3 MDA8, daily NO_2 and NMHCs concentrations in the PRD. The lengths of error bars indicate the corresponding standard deviations. FAC2, the fraction of predictions within a factor of two; MB, mean bias; NMB, normalized mean bias; R, correlation factor.

4. References (of the Supplement)

Chen, X., Liu, Y., Lai, A., Han, S., Fan, Q., Wang, X., Ling, Z., Huang, F., and Fan, S.: Factors dominating 3-dimensional ozone distribution during high tropospheric ozone period, Environ. Pollut., 232, 55–64, https://doi.org/10.1016/j.envpol.2017.09.017, 2018.

Deng, T., Chen, Y., Wan, Q., Zhang, Y., Deng, X., Huang, Y., Dai, G., and Li, F.: Comparative evaluation of the impact of GRAPES and MM5 meteorology on CMAQ prediction over Pearl River Delta, China, Particuology, 40, 88–97, https://doi.org/10.1016/j.partic.2017.10.005, 2018.

Tse, J. W. P., Yeung, P. S., Fung, J. C.-H., Ren, C., Wang, R., Wong, M. M.-F., and Cai, M.: Investigation of the meteorological effects of urbanization in recent decades: A case study of major cities in Pearl River Delta, Urban Climate, 26, 174–187, https://doi.org/10.1016/j.uclim.2018.08.007, 2018.

Yuan, J., Ling, Z., Wang, Z., Lu, X., Fan, S., He, Z., Guo, H., Wang, X., and Wang, N.: PAN–Precursor Relationship and Process Analysis of PAN Variations in the Pearl River Delta Region, Atmosphere, 9, 372, https://doi.org/10.3390/atmos9100372, 2018.